Numerical investigation on effects of side curtain opening behavior on indoor climate of naturally ventilated dairy buildings

Qifeng Li[1,2,3], Chuanxia Yao[1,2,3], Luyu Ding[1,3*], Ligen Yu[1,3], Weihong Ma[1,3], Ronghua Gao[1,3], Wengang Zheng[2,3]

(1. *Beijing Research Center for Information Technology in Agriculture, Beijing 100097, China*;
2. *Beijing Research Center of Intelligent Equipment for Agriculture, Beijing 100097, China*;
3. *Beijing Academy of Agriculture and Forestry Sciences, Beijing 100097, China*)

Abstract: The side-curtain is popular in cattle buildings to regulate indoor climates and ventilation rates by adjusting the opening ratio. It normally had three different adjusting strategies relate to the position of rollers, i.e. central roller (S1), top roller (S2) and bottom roller (S3), which result in different opening behaviors to generate the same opening ratio but different opening positions in the side wall for a full-curtain house. Numerical simulations were conducted using computational fluid dynamics (CFD) to investigate the effects of the eight potential opening behaviors of side curtains on the indoor climates and airflow rates in winter for a typical naturally ventilated dairy house in China when the opening ratio were 8.5% and 17%. Airflow patterns, wind chilled temperature (WCT) and age of air were analyzed in the animal occupied zone (AOZ) by taking reference planes. Openings at the very bottom of side walls had more efficient ventilation due to the younger air age, more effective air disturbing, more uniformly distributed indicators in AOZ. However, it will result in a lower WCT in AOZ although a lower ventilation rate was observed in this case. Openings on the very top of side wall would generate a better thermal comfort in AOZ but with very poor air quality and nonuniformly distributed airflows in the dairy house. S1 was not recommended to the practical application due to the poor indoor climate and the higher cost of the mechanical structure. Based on the comprehensive evaluations of the analytic hierarchy process, the most satisfaction opening positions were at the bottom of the side curtains and the optimized adjusting strategy is S2.

Keywords: thermal comfort, age of air, ventilation rate, computational fluid dynamics, analytic hierarchy process
DOI: 10.25165/j.ijabe.20201305.5805

Citation: Li Q F, Yao C X, Ding L Y, Yu L G, Ma W H, Gao R H, et al. Numerical investigation on effects of side curtain opening behavior on indoor climate of naturally ventilated dairy buildings. Int J Agric & Biol Eng, 2020; 13(5): 63–72.

1 Introduction

Natural ventilation with adjustable curtain sidewalls and the open ridge is popular in housing dairy and beef cattle, especially in China and the USA. Full-curtain or half-curtain are commonly used and the ventilation rate is controlled by opening the sidewall curtain. Based on the natural ventilation principle, the air is driven by the pressure difference across the openings produced by thermal buoyancy and wind forces. The temperature difference between the inlet and outlet of the dairy buildings leads to the difference in air density. The resulting pressure difference forces the airflow to flow from high density to low density. The greater the difference in the center of the inlet and outlet, the greater the pressure difference, thereby enhancing ventilation[1]. For a full-curtain cattle house, it only has a concrete wall around 30 cm above the ground and the sidewall curtain can be adjusted by three different strategies (Figure 1): (1) A central roller generates two openings on the top of the upper side curtain and at the bottom of the lower side curtain (S1, Figure 1a). (2) Two independently controlled curtains at the upper and lower side generate openings at the bottom of each curtain (S2, Figure 1b). (3) Two independently controlled curtains at the upper and lower side generate openings on the top of each curtain (S3, Figure 1c). These different adjustment strategies result in different opening behaviors to get the same opening size with different opening locations.

The location and size of openings lead to different ventilation effects and therefore influence the thermal comfort, air quality, and ventilation rate[2-5]. Previous researches studied indoor climate for various positions of the window opening in residential buildings, but most of them focused on single-sided openings with relatively small size[4]. For the natural ventilation in cattle buildings, it is usually double-sided ventilation and the opening size of the sidewall curtain is very large, although the opening ratio is relatively small. Double-sided ventilation had a higher airflow rate than a single-sided ventilation rate at the same opening area and the large opening would affect the airflow patterns, which consequently alter the thermal comfort and air quality for inside occupants[5,6]. As the existing difference in building characteristics and the thermal requirement for occupants in animal buildings, it is necessary to evaluate the effect of opening behaviors of side curtains on the thermal comfort and air quality of the cattle buildings, guiding the management of the sidewall curtains.

Received date: 2020-03-29 **Accepted date:** 2020-06-17
Biographies: Qifeng Li, PhD, Associate Research Fellow, research interest: precision livestock farming, Email: liqf@nercita.org.cn; **Chunxia Yao,** Master, Engineer, research interest: ventilation and environmental control in animal production systems, Email: yaocx@nercita.org.cn; **Ligen Yu,** PhD, Associate Research Fellow, research interest: precision livestock farming, Email: yulg@nercita.org.cn; **Weihong Ma,** PhD, Assistant Research Fellow, research interest: precision livestock farming, Email: mawh@nercita.org.cn; **Ronghua Gao,** PhD, Associate Research Fellow, research interest: precision livestock farming, Email: gaorh@nercita.org.cn; **Wengang Zheng,** PhD, Research Fellow, research interest: precision livestock farming, Email: zhengwg@nercita.org.cn.
***Corresponding author: Luyu Ding,** PhD, Senior Engineer/Assistant Research Fellow, research interest: gas emission and environmental control in animal production systems. No.11 Shuguang Garden Middle Road, Haidian District, Beijing. Tel/Fax: +86-10-51503855, Email: dingly@nercita.org.cn.

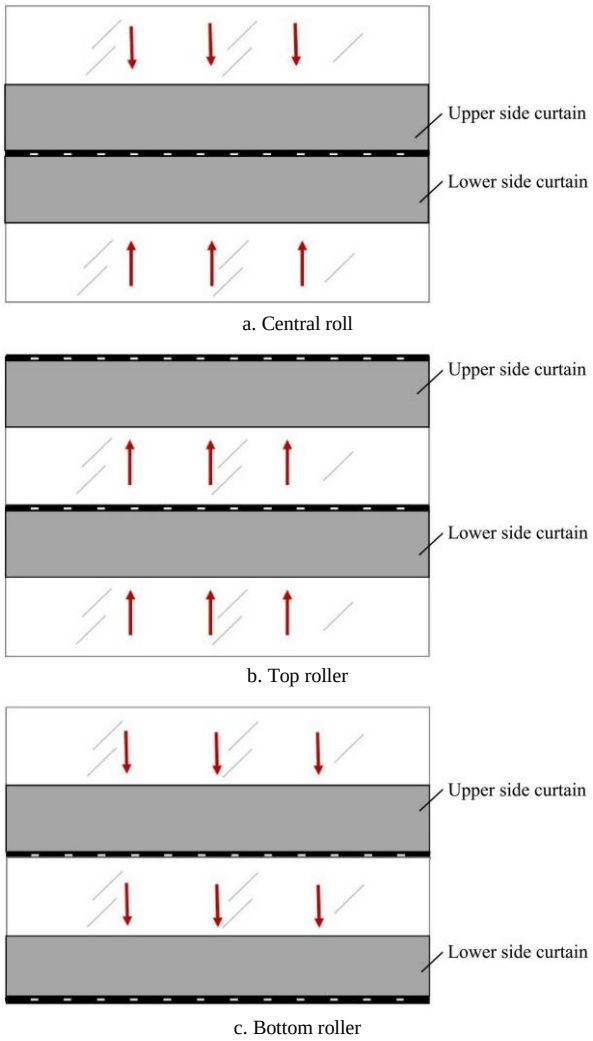

Figure 1 Different adjustment strategies of the full side curtain for cattle buildings

Computational Fluid Dynamics (CFD) is increasingly used to study airflow and thermal environment in livestock building with less cost of time and labor resources[7]. Li et al.[8-10] simulated the pig convective heat transfer process based on CFD and deeply studied the influence of turbulence model, mesh size and mesh generation method on the simulation accuracy of CFD, showing the high accuracy and reliability of the CFD method. It allows full control of the boundary conditions and provides an efficient parametric analysis of different configurations or conditions[11,12]. Guidelines had been summarized for quality control of CFD modeling in livestock buildings which increased the accuracy and reliability in modeling large opening situations and making it to be a popular tool in studying ventilation and indoor climate of naturally ventilated animal houses. For example, Norton et al.[13] compared the performance of ventilated cladding and space boarding on ventilation efficiency and thermal environment of naturally ventilated calf building with different eave opening conditions through CFD modeling. Yi et al.[14] investigated the effects of open ratio and open location on the discharge coefficient of wind-driven naturally ventilated dairy barns. In summer, it is usually fully open of the sidewall curtains to obtain a high airspeed in naturally ventilated dairy buildings. While in winter, the opening of the sidewall curtains is reduced manually according to outdoor climate and artificial experience for heat preservation and preventing cold stress. Lacking scientific guidance, this makes inadequate ventilation and poor indoor air quality in dairy buildings in winter[15].

Thus, the objective of this study is to investigate the impacts of opening behaviors of side curtain on the indoor climate and ventilation rate of naturally ventilated dairy houses in winter by the means of CFD modeling, compare the thermal environment and ventilation efficiency of the three adjusting strategies of side curtain (S1, S2 and S3), and give a recommendation for the adjusting strategy or opening behavior of side curtains in winter application.

2 Materials and methods

2.1 Experimental dairy house and field measurement

A commercial free-stall dairy cattle house with two side full-curtain in Beijing of China was used in this study. It is 92 m long, 28 m wide, 3.5 m eave high, 6.3 m ridge high and stocks 235 milking cows. The house is light-weight steel building structure and solid concrete floor type with external building envelopes of 75 mm thick (100 mm for roof) metal skinned polystyrene sandwich panels. The layout of the dairy cattle house is shown in Figure 2. It has two feeding aisles, a 0.5 m wide ventilation tower in the ridge, 15 entrances/exits of different sizes and 4 large-size side opening. The side openings are 32 m long and 3.14 m tall with a ledge of 0.3 m from inner ground elevation. Each side opening is controlled by two jointly regulated curtains through S2 and generates two sub-openings with a maximum size of 32 m×1.12 m like Figure 1b.

The full-scale CFD model of the experimental cattle house was established for numerical simulation and field measurements were conducted in summer (July 6-14, 2019) for model validation. Air temperature and humidity were logged at 9 locations (Figure 2b, T1-T9) at a height of 2 m by recorders (Apresys 179A-TH, Apresys Inc., Los Angeles, USA) every 5 min. Indoor airspeeds were logged every 1 min by 9 online hot-wire anemometers (XL62WR1ID4, China) at the same location of measuring air temperature and humidity when the fans were open or closed. An infrared thermal imager (FLIR A30, FLIR Systems Inc., USA) was used to obtain the temperature of the inner building surface. Background environmental conditions including air temperature, relative humidity, wind speed, wind direction, radiation, rainfall and evaporation were logged by a weather station (WS1800, China) located at an open space without shielding objects and about 150 m away from the experimental cattle house. The three-dimensional air velocities in the dairy house were measured in a frequency of 20 Hz by ultrasonic anemometers (Wind Master, Gill Instruments Ltd, Hampshire, UK) in the height of 1.25 m at A1 and A2 locations which are shown in Figure 2b. The three-dimensional air velocities were measured during a relatively stable outdoor flow field for at least half an hour in three consecutive days and used for the grid independency analysis.

2.2 CFD model details

2.2.1 Computational geometry and boundary conditions

CFD simulations were carried out based on a full-scale dairy building model with the basic geometry shown in Figure 3a. Cow models were created combining measured dimensions with the simplified model[16]. The neck straps were neglected for model simplification. Turbulence fans in the building were also neglected as it's mainly to investigate the indoor climates in winter and validations were also made when the fans were turned off in this study.

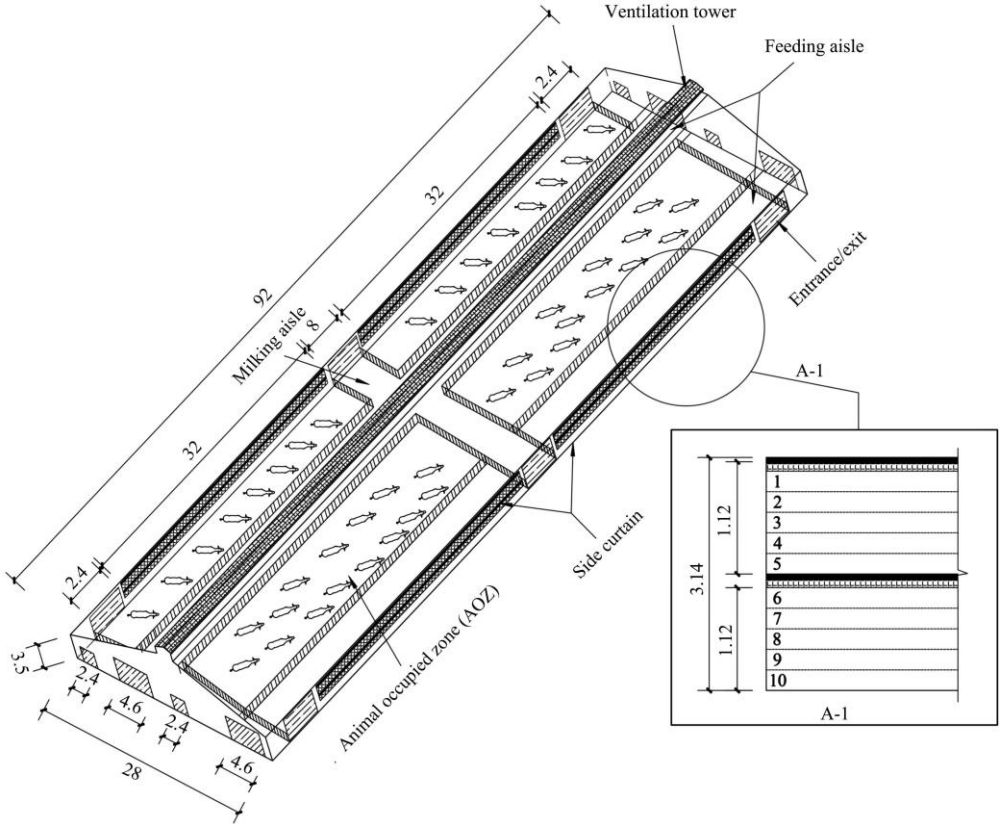

a. Layout of the cattle house

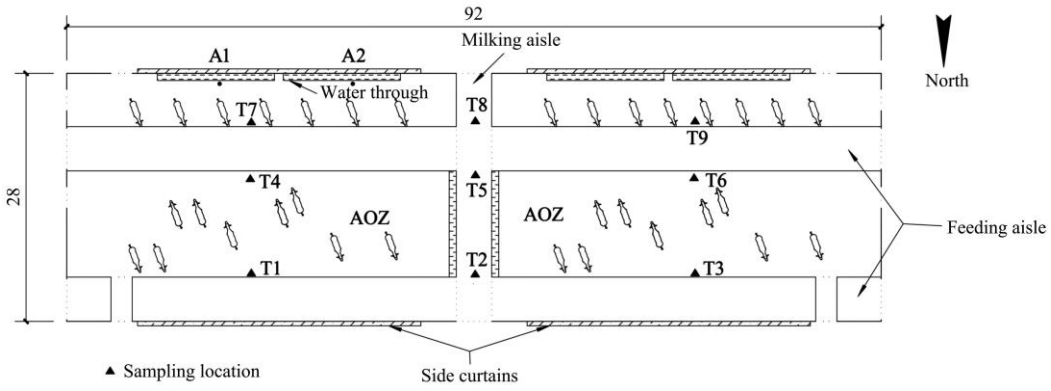

b. Sampling locations

Note: Number 1-10 indicates the different opening positions of the sidewall curtains at a basis opening ratio of 8.5% for each.

Figure 2 Layout of the commercial cattle house and sampling location of air velocity and temperatures

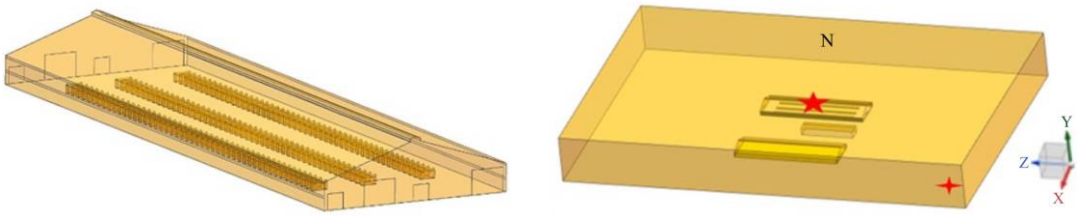

a. Geometry model b. Computational domain

Target dairy building Meteorological station

Figure 3 Geometry model of the simulated dairy building (a) and entire computational domain (b) in CFD modeling

Considering the influence of the adjacent buildings around the target dairy house in a real situation, two adjacent buildings with side walls next to the target dairy building was included in CFD modeling (Figure 3b). For the case with multiple buildings in natural ventilation, the size of the entire computational domain was recommended as 5H from the horizontal boundary of the calculation domain to the target dairy building, 8H from the incoming flow boundary to the windward side of the building and 15H from the leeward side of the building against the incoming flow to ensure the full development of the building wake area, where H is the ridge height of target dairy building[17]. Different prevailing wind speed and direction were observed in summer (July of 2019) and winter (December of 2019) from the experimental dairy farm (Figure 4). Field measurements for model validation were conducted in summer while simulations were conducted for winter cases to evaluate the indoor climate of different opening

behaviors. Thus, taking the target dairy house and the surrounding buildings as a whole target, this research adopts a domain size of 5H×15H×15H away from the whole target for CFD modeling, as shown in Figure 3b.

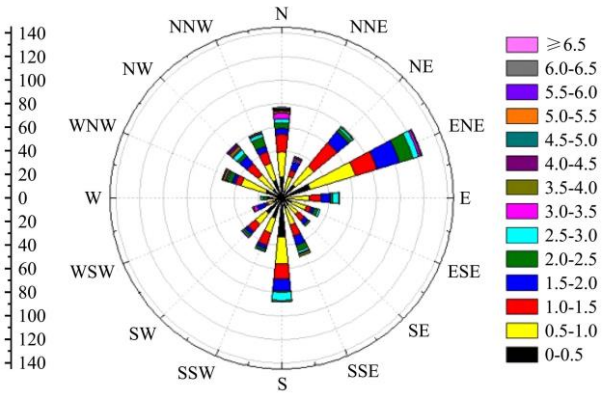

a. Summer

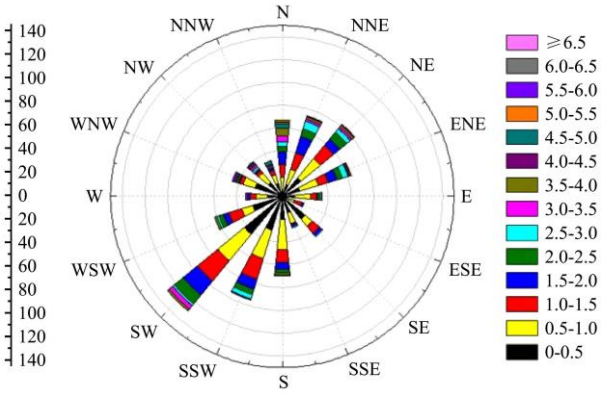

b. Winter

Figure 4 Prevailing wind speed and direction of the experimental dairy farm in summer (a) and winter (b)

The boundary conditions were set according to the measured environmental conditions inside and outside the house when the outside wind speed and direction are relatively stable. The indoor air velocity was monitored when fans were turned off during field measurements in summer. The speed inlet was set at the windward side of the computational domain and the pressure outlet with zero static pressure was set at the downstream boundary of the computational domain. Symmetry planes were used at the top boundary. The interface was used at side curtain opening, the door and top vent in the dairy house. The different opening percentages can be simulated by changing the boundary conditions of the shutter surface.

The heat emitted from the body surface of cows is a major heat source in the dairy house. The heat dissipation of cows was determined using Equations (1) and (2)[18].

$$\varphi_{20\,℃}=5.6m^{0.75}+22Y_1+1.6\times10^{-5}P^3 \quad (1)$$

$$\varphi_{tot}=\varphi_{20\,℃}(1+4\times10^{-5}(20-t)^3) \quad (2)$$

where, $\varphi_{20\,℃}$ is the total heat dissipation from an animal under thermoneutral conditions at 20 ℃, W; φ_{tot} is the total heat dissipation from an animal at a certain air temperature of t, W; m is body mass, kg; Y is milk production, kg/d; P is days of pregnancy.

The heat dissipation of cows in CFD modeling is defined by setting the body surface as a heat source. In this study, the air temperature recorder can obtain the average temperature at different times in the summer and winter inside the dairy building. The average inside temperatures was used to correct the initial heat dissipation of the cows in different seasons in the model, and the cows' heat dissipation is assumed to be a constant value in the calculation process. Other remaining surfaces were simulated as no-slip walls with different conductivities.

2.2.2 Mesh details and numerical solution procedure

The geometry and mesh were created in ICEM CFD (ANSYS 15.0, PA, USA), and the mesh was imported to Fluent for CFD simulation. As shown in Figure 5, the unstructured tetrahedral mesh was used in this study. The minimum size of the mesh was 32 mm and the surface of the cows was encrypted. A grid independence analysis was conducted to ensure that the resolution of the mesh not influencing the results. Three resolutions of the mesh, which were coarse mesh (4.7 million), medium mesh (5.68 million) and fine mesh (8.7 million), were checked in each case with the average environmental conditions. The average three-dimensional air velocities of A1 and A2 are 0.371 m/s, 0.392 m/s, 0.394 m/s, 0.400 m/s for the coarse mesh, medium mesh, fine mesh and measurement, respectively. Medium mesh was selected as the optimal grid size because it provided similar accuracy to fine but required less computation time.

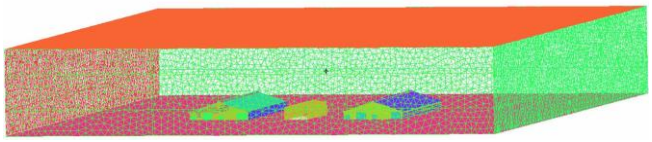

Figure 5 Mesh of entire computation zone

A Re-Normalisation group (RNG) k-ε turbulence model was used to determine turbulence effects because it has been suggested to be more accurate compared to the standard k-ε model when applied to indoor airflow simulation. In addition, the accuracy of LES should be sufficient but normally has higher requirement on meshing and computation power. A full-scale dairy building was used in the simulation which results in relatively large size of the computational model in this study. The excessively fine grids require a very large quantity of the grids, leading to a very long process of calculation[19-21]. The finite volume method was used as the discrete method of the governing equation, and the SIMPLEC algorithm was used for the pressure-speed coupling. The kinetic energy and turbulent flow energy were selected in the second-order upwind style.

2.3 Case study

In winter, side curtains of the dairy building were opened to enhance the ventilation and improve the environment. However, in order to balance the insulation effect of the dairy building, the opening of side curtains is generally small. To evaluate the impacts of opening behaviors of side curtain on indoor climate, numerical simulations were conducted at eight potential operations of side curtains which combined different curtain adjustment strategies at opening ratios of 8.5% and 17%. The opening ratio of the side curtain is defined as the ratio between the actual opening area of two sub-opening generates from the upper and lower curtains and the area of the side wall where the curtains located. Normally, the opening ratio of the dairy building would be less than 50% in most cases of wintertime in northern China and an opening ratio smaller than 10% is treated as a small opening[22]. The different operations generate openings at different positions in the side wall. The maximum size of two sub-openings was divided into 10 pieces and numbered as 1-10 (Figure 2) for a better explanation of the opening positions.

CFD simulations were conducted to compare the thermal comfort, ventilation rate and air quality at different opening behaviors at the outdoor temperature of −9 ℃, wind speed and

direction of 1.3 m/s and 33.7 ° (Northeast). The given boundary condition was selected based on the prevailing wind conditions and daily minimum air temperature in the experimental dairy farm obtained by the weather station in winter (December of 2019) because the opening size of side curtains are often adjusted in cold seasons for heat preservation and raising indoor temperature while the maximum opening size of side curtains are more often used in summer or transitional seasons in practical situation. To verify the reliability of the developed CFD models, simulations were conducted at the maximum opening size with adjustment strategy S2 at the outdoor temperature of 30.4 ℃, wind speed and direction of 2.4 m/s and 148.9 ° (Southeast), as with the summer conditions in-field measurement.

Table 1 Detailed opening behaviors of side curtains simulated in this study

Case No.	Opening ratio	Adjustment strategy	Opening behavior	Position of opening
OC1	8.5%	S3	Open the upper curtain only	1
OC2	8.5%	S2	Open the upper curtain only	5
OC3	8.5%	S2	Open the lower curtain only	10
OC4	17%	S3	Open the upper curtain only	1, 2
OC5	17%	S3	Open both upper and lower curtain to the same size of sub-opening	1, 6
OC6	17%	S1	Open both upper and lower curtain to the same size of sub-opening	1, 10
OC7	17%	S2	Open the lower curtain only	4, 5
OC8	17%	S2	Open both upper and lower curtain to the same size of sub-opening	5, 10

Air temperature and velocity have a joint effect on the thermal comfort of the animal. Wind chill temperature index (WCT), which can be calculated by Equation (3), is a commonly used index to assess the cold stress of livestock in winter when the air temperature is lower than 10 ℃[23]. In this study, WCT was calculated based on the simulated temperature and velocities in the reference planes to evaluate their synthesis effects on the thermal comfort of dairy cows in different opening behaviors.

$$WCT = 13.12 + 0.6215t - 13.17v^{0.16} + 0.3965tv^{0.16} \quad (3)$$

where, t is the air temperature, ℃; v is the air velocity, km/h.

The air age was adopted in this study to assess indoor air quality. The transport equation of the air age can be derived according to the tracer gas method:

$$\frac{\partial}{\partial x_j}(u_j \tau_p) = \frac{\partial}{\partial x_j}\left(\Gamma \frac{\partial \tau_p}{\partial x_j}\right) + 1 \quad (4)$$

where, u_j a three-dimensional speed, m/s; Γ is the diffusion coefficient. It can be seen from the above equation that air age is related to flow and diffusion coefficients.

The uniformity index was used to assess the uniformity of distribution of temperatures or air speeds, describing the change of a specified physical quantity on a specified surface, with 1 being the maximum. The area-weighted uniformity index γ_a of the specified field variable Φ is calculated using the following equation:

$$\gamma_a = 1 - \frac{\sum_{i=1}^{n}[(|\Phi_i - \overline{\Phi_a}|)A_i]}{2|\overline{\Phi_a}|\sum_{i=1}^{n}A_i} \quad (5)$$

where, i is mesh surface index with n mesh surfaces; A_t is the surface area; $\overline{\Phi_a}$ which is the average value of the variables of the entire surface:

$$\overline{\Phi_a} = \frac{\sum_{i=1}^{n}\Phi_i A_i}{\sum_{i=1}^{n}A_i} \quad (6)$$

2.4 Comprehensive evaluation of opening behaviors

To make a recommendation for the opening behaviors of side curtains in cold seasons, the analytic hierarchy process (AHP) was adopted to make a scientific and comprehensive evaluation according to the simulated indoor climate under different curtain operations at the opening ratio of 17%. The AHP methodology, which is widely used in solving evaluation problems by constructing a decision-making problem in various hierarchies as goal, criteria, sub-criteria, and decision alternatives[24]. In the structure of the problem as a hierarchy in this study, the overall goal is the satisfied opening operations of side curtains (G) and the decision alternatives are the five operations at the opening ratio of 17% (OC4-OC8). A similar approach was applied for comparing the three operations at the opening ratio of 8.5% (OC1-OC3).

Considering the indoor thermal comfort, air quality, air flow patterns and the temperature distribution, the criteria adopted in the assessment including thermal comfort in AOZ (A1), age of air at the horizontal plane in AOZ (A2), air velocity distributions in AOZ (A3), age of air at the reference vertical plane of downwind (A4), and the uniformity of the temperature distribution at the horizontal plane in AOZ (A5). Based on the requirement of environment control in dairy buildings and the experience of the authors, A1 and A2 have equal importance and are the most important criteria for respect to the overall goal. Comparing with A1 and A2, A3 and A4 have equal importance as well and are less important while A5 is least important respect to the overall goal. These criteria were assigned to a score of 1-9 based on their intensity of importance to make a pairwise comparison. For example, A2 is of moderate importance to A3, and the comparison weight of A2 to A3 is 3 while the comparison weight of A3 to A2 is 1/3. The weight is 1 when two factors have equal importance. Thus, a pairwise comparison matrix can be developed and Table 2 shows the comparison matrix (A) for the criteria layer in AHP. The maximum eigenvalue (λ_{max}), the consistency index of A (CI) and the consistency ratio (CR) were calculated to check the consistency of the comparison matrix is acceptable or not. Matrix A would be adjusted to improve its consistency if CR is not less than 10%[25].

$$\mathrm{CI} = \frac{\lambda_{max} - n}{n - 1} \quad (7)$$

$$\mathrm{CR} = \frac{\mathrm{CI}}{\mathrm{RI}} \quad (8)$$

where, n is the order of comparison matrix; RI is the consistency index of random matrices and it is 1.12 for a fifth-order comparison matrix.

Table 2 Comparison matrix A of criteria

G	A1	A2	A3	A4	A5	Priority vector
A1	1	1	3	3	5	0.3434
A2	1	1	3	3	5	0.3434
A3	1/3	1/3	1	1	3	0.1290
A4	1/3	1/3	1	1	3	0.1290
A5	1/5	1/5	1/3	1/3	1	0.0551
λ_{max}=5.0556, CI=0.0139, CR=0.0124						

Similarly, comparison matrices of decision alternatives were constructed based on the results of CFD simulation. Weights for the criterion layer or the scheme layer to each criterion were calculated by raising the comparison matrix to sufficiently large power and summing over the rows and normalizing to obtain the priority vector. The weight of each opening operation to the target layer G equals the weight of the criterion layer multiplying

the sum of the weight of the scheme layer. Hence, the satisfied opening operations of side curtains after a comprehensive evaluation can be according to the weight of each opening operations to the target layer G.

3 Results and discussion

3.1 Validation of CFD model

The performance of the CFD model was evaluated by comparing the simulation results with the field measurements of air velocity, air temperature in the summer case. For validation of the CFD simulation of air velocity, the measured and simulated horizontal air velocities were compared because the air velocity meter was placed perpendicular to the airflow to measure the dominant horizontal airflow.

Statistical parameters including fractional bias (FB), normalized mean square error (NMSE), geometric mean bias (MG) and geometric mean variance (VG) were used to evaluate the model performance. The model is considered adequate if more than half of the parameters meet the following criteria, which are |FB|<0.3, 0.7<MG<1.3, NMSE<0.25, VG<4, 0:5<FAC2<2[26].

The comparison between the simulation and measured results in field measurements is shown in Figure 6, and the statistical parameters evaluating the model performance is presented in Table 3. It can be seen from Figure 6 that the simulated temperature is slightly higher than the measured temperature. This may be because the cows in the house go out and milking from time to time during the filed test, resulting in the actual number of cows in the house is lower than the number of cows placed in the simulation. Good agreements were observed between the simulated and measured results for air velocity and temperature which the developed CFD model can adequately predict indoor airflow and air temperature with all criteria being satisfied.

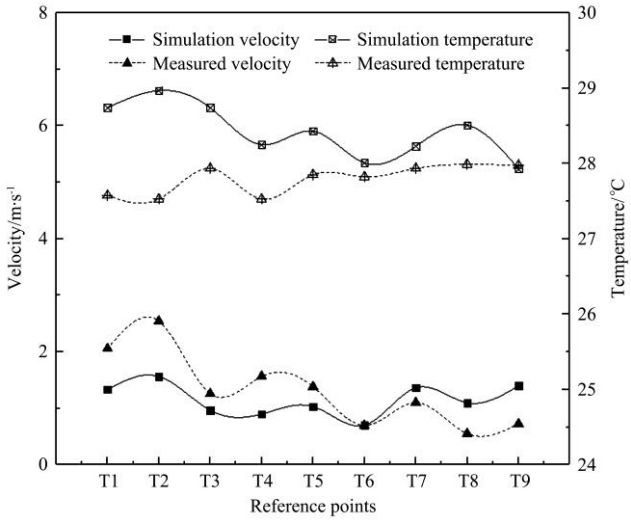

Figure 6 Comparison between measured and modeled air velocities or air temperatures

Table 3 Statistical parameters for the model performance evaluation

	Air velocity/m s^{-1}	Temperature/ ℃
|FB| (<0.3)	0.085	0.021
NMSE (<0.25)	0.236	0.001
MG (0.7-1.3)	0.949	1.023
VG (<4)	1.226	1.001
FAC2 (0.5-2)	1.153	0.978
P-value of Wilcoxon test (>0.05)	0.479	0.400

3.2 Indoor airflow patterns and ventilation rate

The region below 1.5 m was defined as the animal occupied zone (AOZ) in this research. Selecting the horizontal plane at the lying and standing height of cows (y=0.5 m, y=1.5 m) as reference planes, air velocity distributions at y=1.5 m are shown in Figure 7. Table 4 shows the ventilation rate (*VR*), average air velocity as well as the uniformity index of different opening behaviors. Similar air velocity distributions were observed at the plane of y=0.5 m and y=1.5 m. While for several cases where #10 is not opened, the average wind speed at y=0.5 m is slightly higher than that at y= 1.5 m plane. This is due to the airflow disturbance on the y=0.5 m plane mainly comes from the return flow whose direction is south to north in the case of OC1, OC2 and OC7. In the case of OC3, OC6 and OC8, since the bottom opening was open, the direction of air flow at the y=0.5 m plane was consistent with the main wind direction outside. Therefore, the wind speed at y=0.5 m in the OC3 and OC6 case is much greater than y=1.5 m. For OC8, the wind disturbance of y=1.5 is also affected by opening #5 on the lower side, so the wind speed is the largest.

In the winter, the air speed in AOZ is recommended to being lower than 0.4 m/s to avoid cold stress. As can be seen from Figure 7, the overall distribution of air speeds is lower than 0.4 m/s in different cases except for OC3, OC6 and OC8. In these three cases, some high-speed areas have appeared in the barn, thereby increased their average air speed and lowered the uniformity index (Table 4).

Table 4 Averaged air speed (V_m) and uniformity index (U_v) in horizontal reference planes at different opening behaviors

Opening behaviors	y=0.5 m		y=1.5 m		*VR*/m^3 s^{-1}
	V_m/m s^{-1}	U_v	V_m/m s^{-1}	U_v	
OC1	0.16	0.85	0.13	0.84	51.85
OC2	0.16	0.85	0.13	0.80	52.58
OC3	0.42	0.82	0.20	0.80	42.20
OC4	0.27	0.84	0.20	0.83	69.64
OC5	0.17	0.85	0.16	0.76	69.13
OC6	0.38	0.79	0.19	0.78	60.14
OC7	0.23	0.85	0.17	0.84	73.59
OC8	0.22	0.80	0.39	0.73	67.08

Similar average air speed, uniformity index and air distributions were observed between OC1 and OC2 or between OC4 and OC7, which suggests a similar airflow pattern in AOZ at different opening behaviors with the same opening size of the upper side curtain only. From the contour of OC5, it had a lower air speed and a relatively poor uniformity than the other four opening behaviors of the same opening ratio because of the existence of a large area of ventilation dead zone in the southeast corner of the barn. The average air speed of OC3 was close to or even higher than that in OC4-CO8 or in OC1-OC2, which suggests that even a small opening at the bottom of the lower side curtain can cause a relatively high air speed in AOZ.

Average VRs were (47.39±5.79) m^3/s and (67.92±4.94) m^3/s in the dairy house when the opening ratio was 8.5% of the three different opening methods and 17% of the five different opening methods. An 8.5% increase inside opening resulted in a 43.3% higher airflow rate in dairy house. The smaller VRs were observed in OC3, OC6 and OC8, this was due to the less air volume flowed through the top vent in the ridge. Air flowed into the building through the top vent accounts for a larger proportion of the ventilation rate in the house due to the small opening of the

side-curtain in winter. The airflow was close to the wall flowing to the top vent in the case of upper opening, which increases the air flow energy at the top position, thereby increasing the flow through the top vent and eventually leading to a relatively large overall ventilation volume than the lower opening. This suggests that the opening at the bottom of the lower side curtains would result in a lower VR in a dairy house. Moreover, a higher VR in the dairy house was observed when using a central large opening in side wall (OC7), which is due to a relatively large air volume flow through the side curtain opening. More air flowed into the building through side openings when the opening was located in the position of #4, #5, #6. These suggest that the openings at the bottom of the upper side curtains or the top of the lower side curtain would result in a higher VR in dairy house.

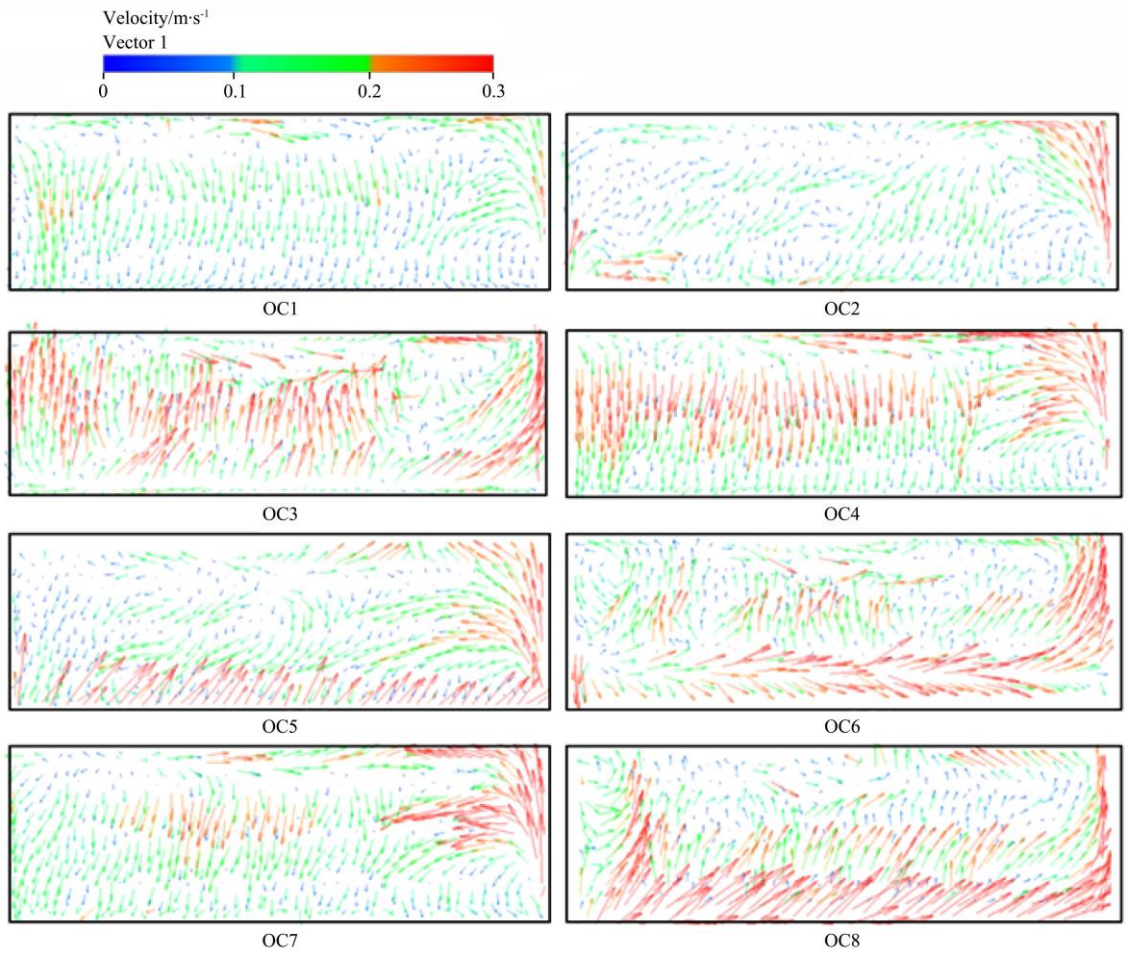

Figure 7 Air velocity distribution in horizontal planes at y=1.5 m at different opening behaviors

3.3 Thermal comfort

Similarly, thermal comfort in AOZ was analyzed by air temperature and WCT at the reference horizontal planes of y=0.5 m and y=1.5 m. Table 5 presents the average air temperature, WCT and the uniformity index at the two reference planes. As all of the uniformity indexes of air temperature in different cases or reference planes were 0.99, the coefficient of variation (CV) was calculated for further reference. Generally, air temperature and WCT distribution were less varied at the reference plane of y = 0.5 m. Figure 8 demonstrates the distribution of WCT for OC1-OC8 at the reference plane of y=1.5 m. Different opening behaviors resulted in a temperature difference in 2 ℃, while would result in a WCT difference in up to 4 because of the joint effect of temperature and air speed in AOZ.

In the cases of a small opening ratio (8.5%), the overall averaged air temperatures were (–7.2 ±1.14) ℃ and (–7.04 ±1.37) ℃ at the plane of y = 0.5 m and y = 1.5 m, respectively. Average air temperature and WCT in AOZ decreased, but the uniformity of their distribution increased when a lower the opening position on the side wall. Although a uniform distribution of temperature can be seen in OC3, it had a much lower WCT in AOZ indicating an adverse effect on the thermal comfort of dairy cows in winter. Air temperature, WCT and their distribution were very close in OC1 and OC2. Compared to OC3, they had a relatively good thermal comfort in AOZ regardless of the nonuniformly distributed air temperature or WCT.

Table 5 Average temperature (T) and its CV, WCT and uniformity index (U_{wct}) in horizontal reference planes at different opening behaviors

Opening behavior	y = 0.5 m/ ℃				y = 1.5 m/ ℃			
	T	CV	WCT	U_{wct}	T	CV	WCT	U_{wct}
OC1	–6.76	21.4%	–5.43	0.86	–6.87	21.4%	–5.04	0.87
OC2	–6.95	18.6%	–5.60	0.87	–7.08	18.6%	–5.07	0.87
OC3	–8.00	–8.4%	–9.04	0.92	–7.16	–8.4%	–6.80	0.91
OC4	–7.52	12.5%	–7.37	0.91	–7.57	12.5%	–6.71	0.91
OC5	–7.10	19.3%	–5.96	0.88	–7.36	19.3%	–5.76	0.87
OC6	–8.32	–8.3%	–8.99	0.91	–8.22	–8.3%	–7.09	0.89
OC7	–7.47	–8.3%	–7.00	0.92	–7.59	–8.3%	–6.41	0.88
OC8	–8.40	12.6%	–9.39	0.91	–8.29	12.6%	–7.39	0.92

In the cases of a large opening ratio (17%), the overall averaged air temperatures were about 0.8 ℃ lower than that of a small opening ratio and which were (–7.76 ±0.94) ℃ and

(–7.81±1.15) ℃ at the plane of y=0.5 m and y=1.5 m, respectively. OC5 had the highest temperature and WCT at two reference planes indicating a relatively good thermal comfort in AOZ at this opening operation. In OC6 and OC8, a much lower temperature or WCT was observed in the windward side of the dairy house and resulted in the lowest average air temperature and WCT compared to other opening operation. This is consistent with the distribution of wind speed.

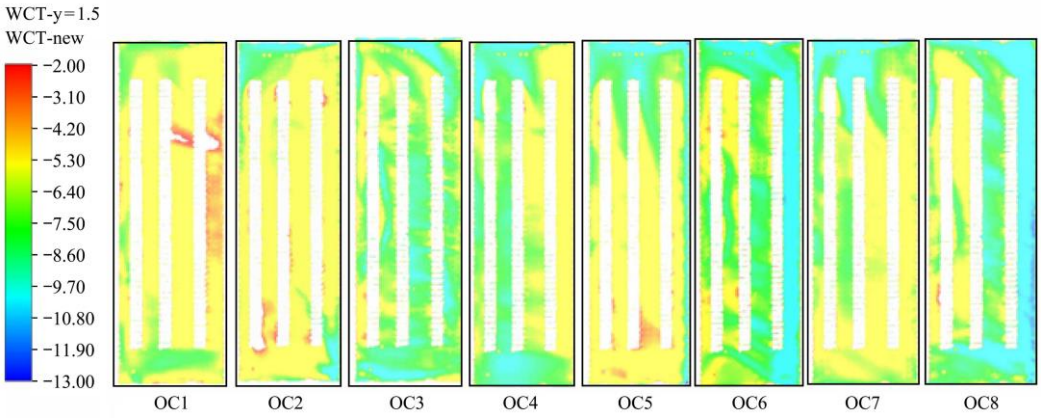

Figure 8 WCT distributions in horizontal planes of y=1.5 m at different opening behaviors

For OC4 and OC7, which is a continuous opening on the upper side curtain, they had a very close average temperature, WCT and thermal distributions. Although OC4 and OC7 had a very close average air temperature to OC5, their average WCT at reference planes was much lower due to their differences in air speeds. Generally, the thermal comfort of OC4 and OC7 in AOZ was not as good as OC5 but better than OC5 and OC8.

3.4 Age of air

The age of air, the time which takes for fresh air from an inlet to reach a designated point inside the structure, can be used to assess the ventilation efficiency and air quality in an agricultural facility[27]. Except for the horizontal planes at the lying and standing height of cows (y=0.5 m, y=1.5 m), the vertical planes of 1/4 building length in the upwind and downwind (z=23 m, z=69 m) were selected as reference planes and Figures 9 and 10 demonstrate the age of air in downwind (z=69 m) and horizontal (y=0.5 m) reference planes.

For the small opening of 8.5%, OC1 had very poor ventilation as the airflow entered the building from the opening on the very top of side curtain and flowed directly along the top surface of the dairy house without causing air disturbance in AOZ. In the case of OC2, the energy was dissipated after air flows enter the house and the leeward side cannot be effectively ventilated. Moreover, the eastern side of the barn is poorly ventilated in OC2 even through its upwind side this may be due to the influence of the adjacent building on the air outlet side. Compared with OC1 and OC2, OC3 had relatively efficient ventilation and good air quality in which the airflow flows along the bottom of side curtain to drive the upper airflow disturbance. As can be seen from Figure 10, there is no ventilation dead zone in OC3.

In the case of O6 and O8, they had a younger air age lower than that of other cases due to the use of bottom opening, #10, which generated an effective disturbance of the airflow on the upper and lower part of the building in the windward side (Figure 9). Comparing the air age distribution of z=23 m and z=69 m, it can be seen that when using the opening located in #1 and #10, OC6 forms small vortices on the upper and lower part of the building in the windward side, disturbing the air. Under the opening conditions of #5 and #10, the upper vortex on the windward side was stronger. At the same time, OC6 and OC8 have the same airflow rules in the house, indicating that the buildings outside the house have little effect on it.

For OC4 and OC7, which only open parts of the upper side curtain, the airflow in the house along the wall surface in both cases did not cause airflow disturbance in AOZ. Comparing the air age distribution of z=23 m, when there is no obstruction of the building outside of z=69 m, the air circulation of OC4 under the opening conditions of #1 and #2 deteriorates, and the airflow velocity of OC7 under the opening conditions of #4 and #5 increases.

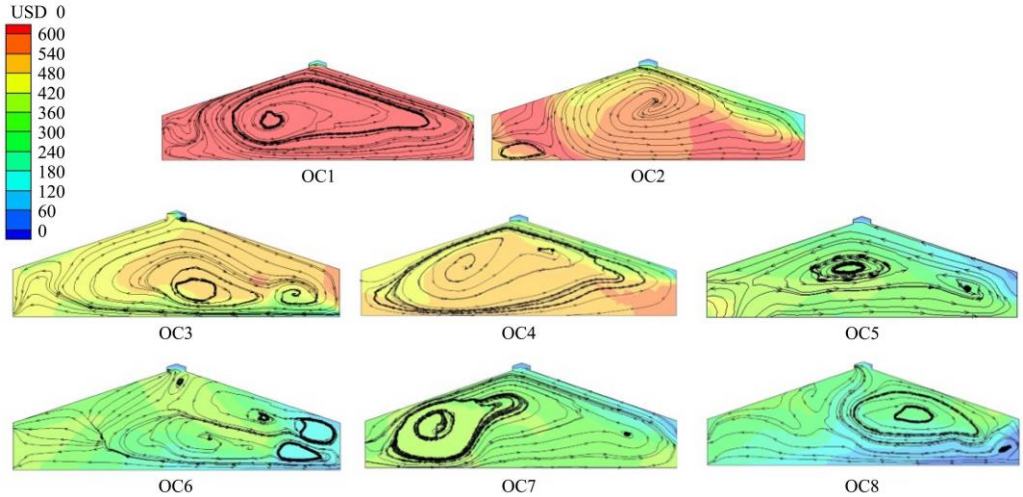

Figure 9 Distribution of air age for the plane of z=69 m at different opening behavior

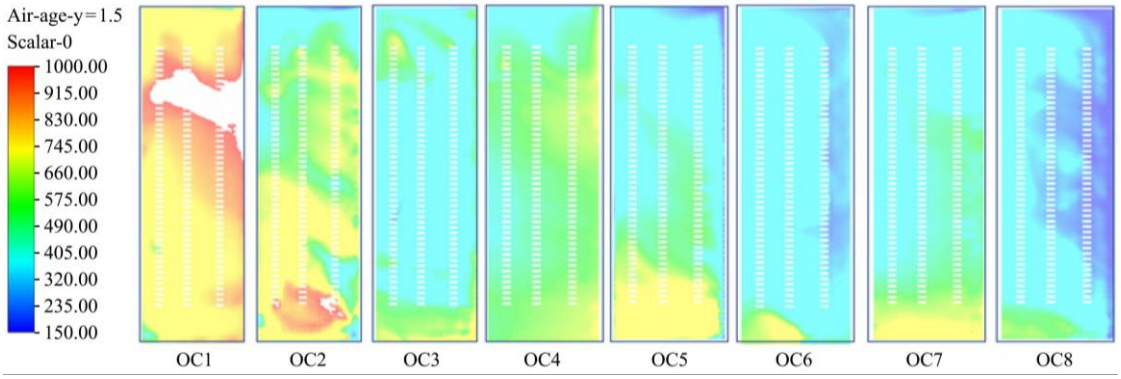

Note: Blank space in the figure indicates that air age here is greater than 1000 s.

Figure 10 Air age distribution at the plane y=1.5 plane under different opening behaviors

In the case of OC5, it was found that the air flow in the upper part of building in the windward side was smooth, but on the z=23 m plane, the airflow was subject to greater resistance when flowing out of the house, resulting in poor air circulation on the leeward side. On the contrary, on the z=69 m plane, the air circulation has been significantly improved.

Compare with all these five opening operations at the ratio of 17%, OC6 and OC8 had a younger air age and more efficient ventilation, followed by OC7 and OC5 had the least efficiently ventilated due to the large ventilation dead zone. The southeast side of the building has poor ventilation due to the influence of neighboring buildings in all cases.

3.5 Comprehensive evaluation of opening behaviors

The satisfaction of opening operations (OC4-OC8) with respect to each criterion (A1-A5) in AHP was compared based on the results of CFD simulation. Considering the thermal comfort in AOZ, OC5 had the highest average WCT at the horizontal planes of y=0.5 m and y=1.5 m in wintertime. The order of the satisfaction of different opening operations to A1 was OC5, OC7, OC4, OC8, OC6 according to the average WCT and air temperature at the reference horizontal planes. However, OC5 had the highest coefficient of variation and lowest uniformity index to average WCT or temperature at the reference planes, which implies a non-uniform distribution of thermal factors. The order of the satisfaction of different opening operations to A5 was OC8, OC4, OC6, OC7, OC5 according to the uniformity index of WCT and air temperature at the reference horizontal planes.

In winter, a relatively small and uniformly distributed air flow is expected in AOZ to alleviate cold stress. Thus, the order of the satisfaction of different opening operations to A3 was OC4, OC7, OC5, OC8, OC6 considering the average air velocity, uniformity index and air distribution especially in the north part of the dairy house at the reference horizontal plane in AOZ. When it comes to air age, OC8 had the most efficient ventilation and the order of the satisfaction of different opening operations to A2 was OC8, OC6, OC7, OC4, OC5 according to their distribution of air age at the reference horizontal plane. Contaminated air tended to accumulate in the downwind section of the dairy house, distribution of air age in the vertical plane of z=69 m was analyzed to evaluate the air quality in downwind. Similar to A2, the order of the satisfaction of different opening operations to A4 was OC8, OC6, OC7, OC4, OC5.

The comparison matrices (Table 6) were developed to calculate the weight of decision alternatives based on their satisfaction with different criteria. Weights of OC4, OC5, OC6, OC7 and OC8 to the target layer G were 0.1845, 0.1749, 0.1611, 0.1836 and 0.2958, respectively. Thus, the order of the satisfaction to the goal was OC8, OC4, OC7, OC5, OC6 considering all the five criteria, OC8 was recommended after a comprehensive evaluation.

Table 6 Comparison matrices of decision alternatives

A1	OC4	OC5	OC6	OC7	OC8	Priority vector
OC4	1	1/2	4	1	2	0.2160
OC5	2	1	7	2	3	0.3980
OC6	1/4	1/7	1	1/4	1/2	0.0554
OC7	1	1/2	4	1	2	0.2160
OC8	1/2	1/3	2	1/2	1	0.1146
λ_{max}=5.009, CI=0.0022, CR=0.0020.						
A2	OC4	OC5	OC6	OC7	OC8	Priority vector
OC4	1	4	1/4	1/2	1/5	0.0925
OC5	1/4	1	1/6	1/5	1/9	0.0363
OC6	4	6	1	2	1/2	0.2732
OC7	2	5	1/2	1	1/3	0.1580
OC8	5	9	2	3	1	0.4400
λ_{max}=5.1122, CI=0.0280, CR=0.0250.						
A3	OC4	OC5	OC6	OC7	OC8	Priority vector
OC4	1	3	7	2	5	0.4319
OC5	1/3	1	3	1/2	2	0.1490
OC6	1/7	1/3	1	1/5	1/7	0.0417
OC7	1/2	2	5	1	3	0.2533
OC8	1/5	1/2	7	1/3	1	0.1242
λ_{max}=5.3206, CI=0.0802, CR=0.0716.						
A4	OC4	OC5	OC6	OC7	OC8	Priority vector
OC4	1	3	1/5	1/3	1/7	0.0634
OC5	1/3	1	1/7	1/5	1/9	0.0333
OC6	5	7	1	3	1/3	0.2615
OC7	3	5	1/3	1	1/5	0.1290
OC8	7	9	3	5	1	0.5128
λ_{max}=5.2375, CI=0.0594, CR=0.0530.						
A5	OC4	OC5	OC6	OC7	OC8	Priority vector
OC4	1	6	2	3	1/2	0.2669
OC5	1/6	1	1/5	1/4	1/7	0.0399
OC6	1/2	5	1	2	1/3	0.1662
OC7	1/3	4	1/2	1	1/4	0.1060
OC8	2	7	3	4	1	0.4210
λ_{max}=5.1220, CI= 0.0305, CR=0.0272.						

Meanwhile, OC6, the opening position special to the adjusting strategy S1 of side curtains, was the least satisfaction to the goal which suggests that S1 was not recommended in practical

application. Similar approach was used for the comprehensive evaluation of indoor climate at the opening ratio of 8.5% (OC1-OC3) and results showed OC2 had the best performance than OC1 and OC3. S2 was recommended as the adjusting strategy for side curtain as both OC2 and OC8 were the opening position consequence to the adjusting strategy S2.

4 Conclusions

Different adjusting strategies (S1-S3) of side curtain induce to different opening behaviors to get the same opening size at different opening locations in the side wall (OC1-OC8). The indoor climate and ventilation rate in the dairy house were affected by the opening behaviors at the same opening ratio. A relatively lower ventilation rate was observed when a bottom opening in the side wall (OC3, OC6) was used while a central opening on the side wall (OC7) tends to increase the ventilation in this study. Compared with other opening operations, OC1 and OC5 had a relatively good thermal comfort in AOZ at the opening ratio of 8.5% and 17% while OC3 and OC8 had more efficient ventilation throughout the dairy house. OC2 and OC8 had a better indoor climate at the opening ratio of 8.5% and 17% taking the average WCT, the uniformity of temperature distribution, age of air in AOZ, age of air in cross-section of downwind and air velocity distribution into consideration. S1 was not recommended in practical application due to its poor indoor climate and higher cost of the mechanical structure.

Acknowledgements

This study was financially supported by the National Key Research and Development Program of China (2018YFD0500702-02, 2018YFE0108500), the Beijing Natural Science Foundation (6194037), the Youth Personnel Project of Beijing Outstanding Talents in 2018.

[References]

[1] Rong L, Bjerg B, Batzanas T, Zhang G. Mechanisms of natural ventilation in livestock buildings: Perspectives on past achievements and future challenges. Biosystems Engineering, 2016; 151: 200–217.

[2] Lago A, Mcguirk S M, Bennett T B, Cook N B, Nordlund K V. Calf respiratory disease and pen microenvironments in naturally ventilated calf barns in winter. Journal of Dairy Science, 2006; 89(10): 4014–4025.

[3] Hassan M A, Guirguis N M, Shaalan M R, El-Shazly K M. Investigation of effects of window combinations on ventilation characteristics for thermal comfort in buildings. Desalination, 2007; 209(1): 251–260.

[4] Prakash D, Ravikumar P. Analysis of thermal comfort and indoor air flow characteristics for a residential building room under generalized window opening position at the adjacent walls. International Journal of Sustainable Built Environment, 2015; 4(1): 42–57.

[5] Liang W, Qin M. A simulation study of ventilation and indoor gaseous pollutant transport under different window/door opening behaviors. Building Simulation, 2017; 10(3): 395–405.

[6] Rong L, Liu D, Pedersen E F, Zhang, G. The effect of wind speed and direction and surrounding maize on hybrid ventilation in a dairy cow building in Denmark. Energy and Buildings, 2015; 86: 25–34.

[7] Guerra-Galdo E H, Estelles Barber F, Calvet Sanz S, Lopez-Jimenez A P. Review of livestock buildings modelled with CFD techniques. International Journal of Energy & Environment, 2017; 8: 405–412.

[8] Li H, Rong L, Zhang G. Study on convective heat transfer from pig models by CFD in a virtual wind tunnel. Computers & Electronics in Agriculture, 2016; 123: 203–210.

[9] Li H, Rong L, Zhang G. CFD prediction of convective heat transfer and pressure drop of pigs in group using virtual wind tunnels: Influence of grid resolution and turbulence modelling. Biosystems Engineering, 2019; 184: 69–80.

[10] Li H, Rong L, Zhang G. Reliability of turbulence models and mesh types for CFD simulations of a mechanically ventilated pig house containing animals. Biosystems Engineering, 2017; 161: 37–52.

[11] Wu W, Zhai J, Zhang G, Nielsen P V. Evaluation of methods for determining air exchange rate in a naturally ventilated dairy cattle building with large openings using computational fluid dynamics (CFD). Atmospheric Environment, 2012; 63: 179–188.

[12] Rong L, Nielsen P V, Bjerg B, Zhang G. Summary of best guidelines and validation of CFD modeling in livestock buildings to ensure prediction quality. Computers & Electronics in Agriculture, 2016; 121: 180–190.

[13] Norton T, Grant J, Fallon R, Sun D W. Assessing the ventilation performance of a naturally ventilated livestock building with different eave opening conditions. Computers and Electronics in Agriculture, 2010; 71(1): 7–21.

[14] Yi Q, Zhang G, König M, Janke D, Hempel S, Amon T. Investigation of discharge coefficient for wind-driven naturally ventilated dairy barns. Energy & Buildings, 2018; 165: 132–140.

[15] Qi S, Liu J, Meng X, Luan D. Study on the winter environment of free-stall barns for lactating cows in Heilongjiang province. Heilongjiang Animal Science and Veterinary Medicine, 2016; 1: 94–96. (in Chinese)

[16] Wu B, Gooch C, Wright P. Verification and recommendations for cooling fans in free stall dairy barns. 2016 ASABE Annual International Meeting. St. Joseph: ASABE, 2016; 162460101. doi: 10.13031/aim.20162460101.

[17] Franke J, Hellsten A, Schlunzen H K, Carissimo, B. The COST 732 best practice guideline for CFD simulation of flows in the urban environment: A summary. International Journal of Environment and Pollution, 2011; 44(1-4): 419–427.

[18] Pedersen S. Heat and moisture production for cattle and poultry on animal and house level. Chicgo, IL, USA, July 28-31, 2002. doi: 10.13031/2013.9390.

[19] Posner J D, Buchanan C R, Dunn-Rankin D. Measurement and prediction of indoor air flow in a model room. Energy and Buildings, 2003; 35(5): 515–526.

[20] Rouaud O, Havet M. Computation of the airflow in a pilot scale clean room using K-epsilon turbulence models. International Journal of Refrigeration, 2002; 25(3): 351–361.

[21] Sun H, Zhao L, Zhang Y. Evaluation of RNG and LES non-isothermal models for indoor airflow using PIV measurement data. Transactions of the ASABE, 2007; 50(2): 621–631.

[22] Seifert J, Li Y, Axley J, Rösslera M. Calculation of wind-driven cross ventilation in buildings with large openings. Journal of Wind Engineering & Industrial Aerodynamics, 2006; 94(12): 925–947.

[23] Angrecka S, Herbut P. Conditions for cold stress development in dairy cattle kept in free stall barn during severe frosts. Czech Journal of Animal Science, 2015; 60(2): 81–87.

[24] Sipahi S, Timor M. The analytic hierarchy process and analytic network process: an overview of applications. Management Decision, 2010; 48(5): 775–808.

[25] Saaty T L. How to make a decision: The analytic hierarchy process. European Journal of Operational Research, 1990; 41(1): 9–26.

[26] Hanna S R, Chang J. Setting acceptance criteria for air quality models. Air Pollution Modeling and its Application XXI, 2012; pp.479–484. doi: 10.1007/978-94-007 -1359-8_80

[27] Kwon K S, Lee I B, Han H T, Shin C Y, Hwang H S, Hong S W, et al. Analysing ventilation efficiency in a test chamber using age-of-air concept and CFD technology. Biosystems Engineering, 2011; 110(4): 421–433.